

Photophysics of 10-Substituted Poly(2-(9-anthryl)ethyl methacrylates)

Marye Anne Fox* and Phillip F. Britt

Department of Chemistry, The University of Texas at Austin, Austin, Texas 78712

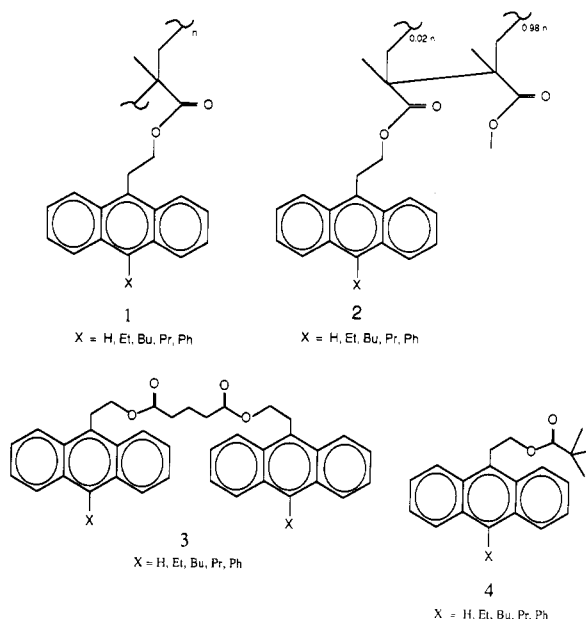
Received January 22, 1990; Revised Manuscript Received April 2, 1990

ABSTRACT: The emission spectra of a series of 10-substituted poly(2-(9-anthryl)ethyl methacrylates) have been studied in solution, frozen glass, and thin films. Excimer fluorescence contributes at least 50% of the observed emission in all homopolymers. Bulky substituents decrease interaction between adjacent and non-adjacent chromophores, thereby reducing self-quenching and increasing the quantum yield of fluorescence. At least two distinct types of excimers could be observed: those formed from interactions of adjacent chromophores and interactions of nonadjacent chromophores at folds or loops in the polymer chain. The contribution of these excimers was found to be dependent on the solvent and the molecular weight of the polymer. Delayed fluorescence spectra indicate that triplet energy migration occurs through the polymer chain until a low-energy trap, e.g., a preformed excimer site, is encountered. The number of traps decreases as the steric bulk of the substituent increases. The lack of monomer fluorescence in the thin films of the homopolymer is indicative of singlet energy migration in the polymers. Strong excimer emission observed from frozen 2-methyltetrahydrofuran glass results from singlet energy migration to an excimer-forming site. A kinetic model for fluorescence quenching by nitromethane is proposed.

Introduction

Expansion of the wavelength sensitivity of stable, wide-band-gap semiconductor electrodes remains a significant problem in photoelectrochemistry.¹ Physical adsorption of monolayer quantities of dye results in high quantum efficiencies for charge injection,² but the low absorptivity of such surfaces renders them impractical. If greater than monolayer quantities are adsorbed, self-quenching dramatically reduces sensitization efficiency. One possible solution to this dilemma involves chromophore-bearing polymers in which interchromophoric interactions are influenced by the polymer's structure and conformational dynamics. We describe in this paper our studies on energy migration in a series of photochemically stable, optically absorptive polymers (poly(2-(10-alkyl-9-anthryl)ethyl methacrylates (1)) and a copolymer 2 in which the monomer unit of 1 is diluted to ca. 2% of the residues. In this family, chromophore interactions are controlled by synthetic manipulation of the 10-substituent, a structural feature to which the observed photophysical properties are quite sensitive. While an increased singlet-state lifetime need not per se enhance photoinduced charge injection, structural modification of the polymer by synthetic manipulation of the monomer chromophores can alter the photophysical properties of the polymer and hence its sensitization efficacy.

The efficiency of singlet energy migration can be probed within such polymeric films via fluorescence spectroscopy and in dilute solution by competitive quenching with nitromethane. We can evaluate the relative contributions of interacting and isolated chromophores in 1 by comparing these measurements with those of the corresponding 10-substituted bis(2-(9-anthryl)ethyl) glutarates (3) and pivalates (4), compounds that have served as monomeric models for the polymers.³ Our goals were to establish the effect of the steric bulk of the 10-substituent on excimer formation and energy migration in the polymer, to probe for triplet energy migration to preformed excimer sites, and to correlate polymer structure with sensitization efficiency in polymeric layers.



Experimental Section

Instrumentation. Proton nuclear magnetic resonance (¹H NMR) spectra were obtained on a Varian EM-390 (90 MHz) or a Nicolet NT-200 (200 MHz) spectrometer in chloroform-*d* solutions. Carbon-13 nuclear magnetic resonance (¹³C NMR) spectra were obtained on a Varian FT-80A (20 MHz) or a GE/Nicolet GN-500 (500 MHz) spectrometer in chloroform-*d* solutions. Chemical shifts are reported in parts per million (ppm) from SiMe₄ (δ 0.0) as an internal standard. Low-resolution mass spectra (MS) and high-resolution mass spectra (HRMS) were obtained on Du Pont 21-491 and (CEC) 21-110 spectrometers, respectively. Melting points were measured on a Fisher-Johns apparatus and are uncorrected. UV-visible spectra were recorded on a Cary 15 or a Hewlett-Packard 8450 or 8451A spectrophotometer. Analytical thin-layer chromatography (TLC) was performed with Sybron/Brinkmann silica gel/UV₂₅₄ plates (0.25 mm thick). Preparative TLC was performed on Analtech silica gel GF plates (20 × 20 cm, 2.0 mm thick). Flash chromatography was performed on Merck silica gel 60 (230–400 mesh). Gel permeation chromatography was carried out with a Waters 6000A solvent delivery system using μ-Styragel columns (7.8 mm i.d. × 30 mm) with methylene chloride or tetrahydrofuran as the mobile phase.

Materials. All reagents and solvents were reagent grade and were checked for impurities by absorption and fluorescence spectroscopy before use. Spectrophotometry grade benzene (MCB) was used without further purification. 2-Methyltetrahydrofuran (MTHF) was passed through active alumina and fractionally distilled from sodium and then lithium aluminum hydride immediately before use. Toluene was distilled from sodium immediately before use. Methylene chloride was distilled from P_2O_5 immediately before use. Acetonitrile (HPLC grade) was fractionally distilled from lithium aluminum hydride.

Fluorescence Spectra. Emission and excitation spectra were recorded at 90° on either a Spex Fluorolog 2 or an SLM Aminco SPF 500 spectrofluorimeter. All solutions were purged with nitrogen and had optical densities <0.05 in a 1-cm cuvette unless otherwise noted. The emission spectra were measured in the ratio mode (to correct for variation in lamp intensity with time) and are corrected for nonlinear response of the photomultiplier tube. The fluorescence quantum yields were measured in benzene relative to 9,10-diphenylanthracene (benzene solution, $\Phi = 0.84$).⁴ When measurements were made in MTHF, corrections were made for the difference in the refractive index of the solvents. Quantitatively reproducible fluorescence quantum yields were obtained when the samples were purged with nitrogen for 20 min or when the samples were degassed on a high-vacuum line (10^{-5} Torr) with six freeze-pump-thaw cycles and sealed with a high-vacuum stopcock. Fluorescence spectra of thin films on glass or SnO_2 were measured by front-face analysis or by placing the sample at a 45° angle to the excitation beam. Delayed fluorescence spectra were measured on an SLM Aminco spectrofluorimeter with a rotating-can accessory.

Fluorescence Lifetimes. Fluorescence decays were recorded by time-correlated single-photon counting.⁵ The light source was a Photochemical Research Associates (PRA) Model 510B thyatron-gated flash lamp operated at 20 kHz, 5 kV, and 0.5 atm of air with a full width at half-maximum of ca. 2.4 ns. The excitation wavelength ($\lambda = 358$ nm) and emission wavelength were selected with two Jobin-Yvon monochromators. The fluorescence decay, measured at right angles to the excitation source, was passed through a $NaNO_2$ filter (cut-off $\lambda < 390$ nm) and detected by a water-cooled Hamamatsu photomultiplier tube. Standard pulse-shaping methods were used for start-stop pulses using a Pacific Precision Instruments Model AD-1261 amplifier-discriminator or a PRA 1718 100-MHz discriminator, a PRA 1703 delay, a PRA 1716 timing discriminator, and a PRA 1701 biased time-to-pulse height convertor. A LeCroy analog-to-digital converter was used to digitize the output into the histogram memory of a LeCroy Model 3500 multichannel analyzer. The detection rate was ca. 1% of the pulse rate needed to discriminate between two photon events. A minimum of 10 000–20 000 counts were collected in each peak channel. The data were transferred to The University of Texas Cyber computer and fit to exponential decay functions using previously described deconvolution techniques to obtain a best fit.³

General Procedure for the Synthesis of 10-Substituted 2-(9-Anthryl)ethyl Methacrylate. A solution of 10-substituted 2-(9-anthryl)ethanol³ (1 equiv) and triethylamine (2 equiv) in THF or toluene (20 mL) was cooled to 0 °C, and methacryloyl chloride (1.25 equiv) was added. The reaction was stirred at 0 °C for 4 h, before being allowed to warm to room temperature and to stir for 18 h. The reaction mixture was then poured into water (30 mL) and extracted with ether (3 × 30 mL). The combined organic layers were washed sequentially with 2 M HCl (3 × 30 mL) and water (1 × 30 mL) and dried over $MgSO_4$. The solvent was removed under reduced pressure, and the residue was purified by flash chromatography.

2-(9-Anthryl)ethyl methacrylate: chromatographed with benzene-hexanes (1.5:1); yield 0.56 g (72%); mp 87–88 °C; 1H NMR 1.87 (s, 3 H), 3.93 (t, 2 H, $J = 7.5$ Hz), 4.48 (t, 2 H, $J = 7.5$ Hz), 5.43 (s, 1 H), 6.00 (s, 1 H), 7.25–7.57 (m, 4 H), 7.83–8.00 (m, 2 H), 8.17–8.37 (m, 3 H).

2-(10-Ethyl-9-anthryl)ethyl methacrylate: chromatographed with benzene-hexanes (1.5:1.0); yield 1.4 g (72%); mp 120–121 °C; 1H NMR 1.38 (t, 3 H, $J = 7.5$ Hz), 1.88 (br s, 3 H), 3.55 (q, 2 H, $J = 7.5$ Hz), 3.93 (t, 2 H, $J = 7.5$ Hz), 4.50 (t, 2 H, $J = 7.5$ Hz), 5.46 (br s, 1 H), 6.03 (br s, 1 H), 7.37–7.60 (m, 4 H), 8.13–8.47 (m, 4 H); ^{13}C NMR (500 MHz) 15.5, 18.3, 21.2, 27.3,

Table I
Molecular Weights of the Homopolymers 1^a

compd	$M_w \times 10^{-3}$	DP ^b	M_w/M_n ^c
1-H(L)	16	26	2.1
1-H(H)	88	120	2.5
1-Et	65	100	2.0
1-n-Bu	180	220	2.3
1-i-Pr	110	140	2.2
1-Ph	150	160	2.7

^a By GPC based on a standard polystyrene calibration curve. ^b Average degree of polymerization. ^c Polydispersity.

64.5, 125.0, 125.0, 125.4, 125.6, 127.5, 128.3, 129.0, 130.2, 136.3, 136.4, 167.6; MS, m/e (% relative intensity): 318 (16), 232 (35), 219 (25), 217 (21), 203 (100), 191 (10), 189 (10), 69 (10), 41 (24); HRMS calcd for $C_{22}H_{22}O_2$, 318.1620; found 318.1626.

2-(10-*n*-Butyl-9-anthryl)ethyl methacrylate: chromatographed with benzene-hexanes (1.5:1.0); yield 1.0 g (71%); mp 91.5–92.5 °C; 1H NMR 1.0 (t, 3 H, $J = 6.9$ Hz), 1.35–2.00 (m, 4 H), 1.91 (br s, 3 H), 3.55 (t, 2 H, $J = 7.5$ Hz), 3.93 (t, 2 H, $J = 7.5$ Hz), 4.50 (t, 2 H, $J = 7.5$ Hz), 5.47 (br s, 1 H), 6.05 (br s, 1 H), 7.37–7.63 (m, 4 H), 8.15–8.50 (m, 4 H); ^{13}C NMR (500 MHz) 14.1, 18.4, 23.5, 27.3, 28.0, 33.5, 64.5, 124.9, 125.1, 125.3, 125.4, 125.6, 127.5, 129.4, 130.2, 135.3, 136.4, 167.6; MS, m/e (% relative intensity) 346 (20), 260 (46), 247 (10), 217 (52), 203 (100), 191 (46), 69 (14), 41 (32); HRMS calcd for $C_{24}H_{26}O_2$, 346.1932; found, 346.1929.

2-(10-(Isopropyl-9-anthryl)ethyl methacrylate: chromatographed with benzene-hexanes (2.5:1.0); yield 0.15 g (63%); mp 138–139 °C; 1H NMR 1.75 (d, 6 H, $J = 7.2$ Hz), 1.93 (s, 3 H), 3.97 (t, 2 H, $J = 7.5$ Hz), 4.37–4.73 (m, 3 H), 5.50 (br s, 1 H), 6.07 (br s, 1 H), 7.27–7.60 (m, 4 H), 8.27–8.53 (m, 4 H); ^{13}C NMR 18.4, 23.0, 27.5, 28.4, 64.5, 124.3, 125.2, 125.6, 125.7, 125.8, 127.9, 129.2, 130.5, 136.4, 140.4, 167.7; MS, m/e (% relative intensity) 332 (43), 246 (71), 233 (22), 231 (48), 218 (22), 215 (26), 203 (100), 191 (23), 332 (43), 246 (71), 233 (22), 231 (48), 218 (22), 215 (26), 203 (100), 191 (23), 178 (10); HRMS calcd for $C_{23}H_{24}O_2$, 332.1776; found, 332.1781.

2-(10-Phenyl-9-anthryl)ethyl methacrylate: chromatographed with benzene-hexanes (1.5:1.0); yield 1.5 g (60%); mp 156.5–157.5 °C; 1H NMR 1.93 (br s, 3 H), 4.03 (t, 2 H, $J = 7.5$ Hz), 4.57 (t, 2 H, $J = 7.5$ Hz), 6.07 (br s, 1 H), 6.50 (br s, 1 H), 7.13–7.70 (m, 11 H), 8.38 (d, 2 H, $J = 9$ Hz); ^{13}C NMR (500 MHz) 18.4, 27.4, 64.5, 124.1, 124.8, 125.7, 127.4, 127.8, 128.3, 129.0, 130.0, 131.2, 131.3, 136.3, 137.1, 139.1, 167.6; MS, m/e (% relative intensity) 366 (28), 280 (100), 267 (49), 252 (36), 203 (46); HRMS calcd for $C_{26}H_{22}O_2$, 366.1620; found, 366.1626.

Synthesis of Polymers. A. Homopolymers. A benzene solution of monomer (10% by weight) and 2,2'-azobis(isobutyronitrile) (AIBN, 1% by weight) was degassed with three freeze-pump-thaw cycles and sealed. The solutions were heated at 60 °C for 40 h in the dark. The polymers were precipitated by pouring the benzene solutions into a rapidly stirred solution of absolute ethanol (20 mL). The white solid was filtered, dissolved in benzene, and precipitated by the dropwise addition of ethanol. This procedure was repeated twice. The polymers were washed with cold ethanol and dried under vacuum: yield 65–73%.

The weight-average molecular weight M_w and the number-average molecular weight M_n (Table I) were determined by gel permeation chromatography (GPC) using Waters μ -Styragel columns (500-, 10^3 -, 10^4 -, and 10^5 -Å pore size) with THF as the mobile phase. A calibration curve was determined with monodisperse ($M_w/M_n < 1.1$) polystyrene standards of molecular weights 4000, 37 000, 110 000, 200 000, and 390 000. The GPC traces were digitized and stored on a HP-85 computer where the calculations were performed. The average degree of polymerization DP ($=M_n/M_0$, where M_0 is the molecular weight of the monomer) represents the average number of monomer units in a polymer chain. The polydispersity, calculated from M_w/M_n , depends on the breadth of the molecular weight distribution curve. High and low molecular weight fractions of 1-H were generated, designated as 1-H(L) for the light fraction and 1-H(H) for the heavy fraction.

Table II
Molecular Weights of the Copolymers 2^a

compd	$M_n \times 10^{-3}$	mol % of anthracene ^b
2-H	58	2.0
2-Et	68	2.1
2- <i>n</i> -Bu	78	2.1
2- <i>i</i> -Pr	70	1.5
2-Ph	75	2.0

^a By GPC based on polystyrene calibration curve. ^b By UV analysis.

B. Copolymers. A benzene solution of methyl methacrylate (5% by weight), 10-substituted 2-(9-anthryl)ethyl methacrylate (0.3% by weight), and AIBN (0.03% by weight) was degassed with three freeze-pump-thaw cycles and sealed. The polymers were heated at 60 °C for 24 h in the dark. The polymers were purified by precipitation (3 times) by the slow addition of ethanol. Molecular weight (M_n) was determined by GPC as discussed above (Table II).

Thin Films. Thin films of the polymers were deposited on glass slides or SnO₂ electrodes by spin-coating. Microscope slides (1 × 2 cm) were soaked sequentially in alcoholic KOH (2 M), concentrated H₂SO₄, water, 2-propanol, distilled acetone, and benzene. The slides were dried at 130 °C for 12 h and placed in a desiccator. Antimony-doped tin oxide coated glass (SnO₂: 1 × 2 cm, highly conducting NESA glass, PPG industries) was soaked in alcoholic KOH (2 M) followed by copious rinsing with deionized water. The electrodes were washed sequentially with 2-propanol, distilled acetone, and benzene, dried at 130 °C for 12 h, and placed in a desiccator. The plates were attached to a Pine Instruments Co. analytical rotator with double-stick tape, and two or three drops of a *p*-xylene solution of the polymers (1–7% by weight) were applied as the plate was rotated at 2000–4000 rpm. The uniformity of the films was determined by UV spectroscopy by measuring the optical density (OD) (λ_{\max}) at 6–8 different places on the electrode ($\pm 10\%$). The OD of the film was controlled by the concentration of the stock solution. For a given stock solution, the OD of the films was reproducible to $\pm 15\%$ except for absorption measurements below 0.10 ($\pm 20\%$).

Fluorescence Quenching. A dilute benzene solution (3 mL, $< 10^{-5}$ M, OD < 0.10) of compound was pipetted into a quartz cuvette. Benzene-saturated argon was bubbled through the solution for 20 min before the cuvette was sealed. A deoxygenated solution of nitromethane was added to the cuvette via a microliter syringe. Argon was bubbled through the sample for an additional 3–5 min to ensure thorough mixing. Fluorescence quenching was determined from either the intensity of the emission at a peak or the integrated intensity over the spectrum; each method gave similar results. For the homopolymers, monomer intensity was monitored at the 0,0 band and excimer emission was monitored at its emission maximum or at a wavelength where the monomer does not emit. The chromophores were excited at 385 or 395 nm to avoid the excitation of the quencher. At the highest concentrations of quencher, no new bands were observed in the absorption or fluorescence spectra.

Photostability. The photostabilities of 1 were investigated by irradiation ($\lambda > 330$ nm) of dilute degassed solutions (10^{-4} M) at 30 °C. The disappearance of the anthryl chromophore was measured by UV spectroscopy (at the 0,0 and 0,1 bands) after 2, 24, 72, and 288 h of irradiation.

Results and Discussion

Absorption Spectra. The absorption spectrum of the parent homopolymer 1-H is very similar to that of the diluted copolymer 2-H. The vibrational bands for the homopolymer are broader and red-shifted 1–2 nm from that of the copolymer. The molar extinction coefficients for the long-wavelength transitions of the homopolymers are only slightly smaller ($\pm 2\%$) (Table III) and are very similar to those of the pivalate models 4. Thus, ground-state interactions between the closely spaced chromophores bearing bulky substituents are inhibited. The spectral shifts most likely result from the interactions

between the transition dipole moments (Coulombic interactions) of two adjacent molecules.⁶ Since the magnitude of these interactions is proportional to the oscillator strength, the short-wavelength transitions in the anthracene chromophore ($\lambda = 260$ nm, $\epsilon \approx 10^5$) should show the largest spectral change. The short-wavelength transitions are substantially broader and slightly red-shifted compared to those in the copolymer. The shoulder at 254 nm in 2-H appears as a resolved peak at 253 nm in the homopolymer 1-H. The molar extinction coefficient of this band is $\approx 40\%$ smaller than that of the copolymer but with a large increase in the width of the absorption band. Similar spectral alterations were observed for the “broken dimers” of glutarate 3-H⁷ where two anthryl groups are held in close proximity by a rigid matrix.

Fluorescence Spectra. A. In Fluid Solution and Frozen Glasses.

(1) 1-H. The fluorescence spectrum of 1-H in benzene is compared to 2-H in Figure 1. The fluorescence of the homopolymer is dominated by excimer emission, $\lambda_{\max} = 525$ nm. The excimer/monomer contribution (I_D/I_M) was estimated from the ratio of intensities of emission at its maximum for the excimer (I_D) and at the 0,0 band for the isolated chromophores (I_M) (Table IV). The wavenumber difference between the 0,0 band of fluorescence and the maximum of excimer emission $\Delta\nu$ (6528 cm⁻¹) is much larger than $\Delta\nu$ for the intramolecular excimer of glutarate 3 ($\Delta\nu = 3809$ cm⁻¹)⁷ but very similar to that for the intermolecular excimer of 9-methylanthracene ($\Delta\nu = 6850$ cm⁻¹).⁸ The blue spectral shift of the monomer fluorescence probably indicates the presence of isolated chromophores that cannot reach the geometry required to form an excimer within their excited-state lifetimes, since coiling of the polymer chain restricts the conformational mobility of the pendant groups. A similar explanation has been used to explain the fluorescence decay behavior of poly(1-naphthylalkyl methacrylates).⁹ Similar effects are also observed in the 10-substituted 1.

The quantum yields of fluorescence Φ_F of substituted 1 are ≈ 4.5 times smaller than those of the analogous 2 (Table IV). This indicates that the high local concentration of chromophores in 1 provides a mechanism for fluorescence quenching, presumably through the excimer.

The excitation and emission spectra of the copolymers 2 and the corresponding 10-substituted pivalates 4 are identical (Table IV), indicating that the chromophores are isolated. The quantum yields of fluorescence of 2 and 4 are also identical within experimental error. Thus, the polymer backbone is inert and does not lead to enhanced fluorescence quenching. Somewhat lower quantum yields of fluorescence are observed for 1, 2, and 4 in MTHF, since the rate constant for fluorescence k_{FM} is dependent on the refractive index of the solvent.¹⁴

Spectral shifts can also be observed between high and low molecular weight fractions of 1-H. As the molecular weight increases, polymer-polymer interactions become dominant and the polymer chain contracts, increasing excimer formation between nonadjacent chromophores. The excimer contribution to the fluorescence spectrum of low molecular weight 1-H(L) is much lower than in high molecular weight 1-H(H) in MTHF (Figure 1). 1-H(L) has a distinct band for the excimer at 525 nm, and the maxima of the monomer bands are blue-shifted to the same positions as in the corresponding pivalates. Such molecular weight effects have been reported for poly(naphthyl methacrylate),¹⁰ poly(1-vinylnaphthalene),¹¹ poly(2-vinylnaphthalene),¹² and polystyrene.¹³ Therefore, there are at least two distinct excimer-forming sites in 1-H, the relative

Table III
Absorption Spectral Data for 10-Substituted 2-(9-Anthryl)ethyl Pivalate and Methacrylate Polymers

compd	substituent									
	H		Et		<i>n</i> -Bu		<i>i</i> -Pr		Ph	
	λ , nm	$\epsilon \times 10^{-3}$, M ⁻¹ cm ⁻¹	λ , nm	$\epsilon \times 10^{-3}$, M ⁻¹ cm ⁻¹	λ , nm	$\epsilon \times 10^{-3}$, M ⁻¹ cm ⁻¹	λ , nm	$\epsilon \times 10^{-3}$, M ⁻¹ cm ⁻¹	λ , nm	$\epsilon \times 10^{-3}$, M ⁻¹ cm ⁻¹
4a	386	9.80	398	12.2	398	122	398	9.72	394	13.1
	380	sh ^d	392	sh	393	sh			389	sh
	366	9.80	376	11.5	378	11.8	378	10.2	374	13.6
	348	6.03	358	6.93	358	6.68	360	6.1	356	8.10
	340	3.06	342	2.96	342	2.82	340	3.63	340	3.70
	316	sh	324	sh	324	sh			323	sh
	256	116	262	120	262	125	c	c	260	125
	255	sh	255	sh	253	sh			250	sh
	220	11.7	222	13.4	222	14.0	c	c	224	sh
1^b	392	9.10	402	10.8	402	10.6	402	8.98	400	13.00
	370	9.80	380	11.2	380	11.0	380	9.40	378	14.0
	352	6.33	362	6.92	362	6.50	362	5.75	360	8.57
	336		344	2.87	344	2.80	344	2.92	342	4.04
	262	84.1	266	84.2	266	85.4	266	70.2	264	86.5
	254	80.5	258	77.1	258	78.6	260	63.0		

^a In hexanes. ^b In CH₂Cl₂. ^c Not measured. ^d sh = shoulder.

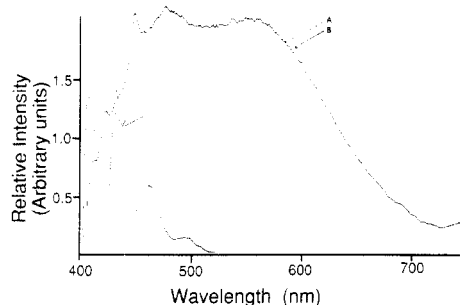


Figure 1. Fluorescence spectra of 1-H(H) (A) and 2-H (B) in benzene (ca. 10⁻⁴ M) under nitrogen at room temperature. Excitation at 380 nm.

Table IV
Quantum Yields of Fluorescence of 1, 2, and 4 in Dilute Benzene^{a,b}

subst	Φ_F			I_D/I_M^c	$\Delta\nu$, cm ⁻¹
	1	2	4		
H ^d	0.12	0.53	0.52	2.4	6528
Et	0.35	0.76	0.78	2.8	6298
<i>n</i> -Bu	0.35	0.73	0.83	2.2	5859
<i>i</i> -Pr	0.77	0.88	0.87		
Ph	0.76	0.84	0.85		

^a Nitrogen-saturated solutions at room temperature. ^b All measurements repeated 3–6 times. Error $\pm 10\%$. ^c Ratio of maximum intensity of the excimer emission I_D to intensity of the 0,0 band (monomer emission) I_M . ^d High molecular weight fraction.

predominance of which depends on the molecular weight of the polymer and on the solvent.

A coiled polymer can form two kinds of excimers: (1) between nearest neighbors and (2) between different segments of the polymer chain. The excimer formed between nearest neighbors is expected to be similar to that observed in glutarate 3, which was identified as a strained excimer,⁷ since its emission maximum was blue-shifted and its Stokes shift was smaller than that of 9-methylanthracene.⁸ Excimers formed through segmental diffusion of the polymer chain could be unstrained and would then have spectral properties similar to those of intermolecular excimers. The relative abundance of these two excimers may be solvent dependent. In a good solvent, such as benzene, the polymer chain is extended to maximize polymer-solvent interactions and excimer formation can occur mainly between adjacent chromophores. In a poor

solvent, such as MTHF, the polymer chain contracts and coils to maximize the polymer-polymer interaction.

The fluorescence spectrum of 1-H(H) in MTHF at 77 K is not a mirror image of its excitation spectrum. The vibrational bands of the spectrum are broadened and red-shifted relative to those of pivalate 4-H at 77 K, indicating that the chromophores are close enough in the ground state to form weak excimers without significant movement at preformed excimer sites.¹⁵ The excitation spectrum is independent of monitoring wavelength and does not show a new absorption from these ground-state interactions. Similar results have been reported for poly(9-anthrylmethyl methacrylate)¹⁶ where the room temperature spectrum is nearly identical with that in frozen glass. Similar spectral changes were observed in the emission spectrum of poly(2-naphthylalkyl methacrylate) as the alkyl chain increased from methyl to ethyl to propyl.¹⁷

(2) 1-Et. The fluorescence spectrum of 1-Et in benzene at room temperature is similar to that of 1-H, exhibiting emission maxima red-shifted ca. 4 nm from the isolated chromophores in 2-Et. The observed fluorescence is dominated by excimer emission at 553 nm, $\Delta\nu = 6298$ cm⁻¹. The ratio I_D/I_M is 2.82 in benzene and 3.93 in MTHF, a result of coiling of the polymer chain in the poorer solvent. The quantum yield of fluorescence of 1-Et is lower in MTHF than in benzene (0.23 vs 0.35, respectively), indicating that excimer formation enhances fluorescence quenching. The quantum yield of fluorescence of 1-Et is approximately half that of 2-Et (Table IV). A comparison of the ratio of the Φ_F of homopolymer to Φ_F of copolymer for the ethyl-substituted polymer with the parent (1-H/2-H = 0.23 and 1-Et/2-Et = 0.45) indicates that the efficiency of emission increases by a factor of 2 with ethyl substitution. Therefore, the introduction of an ethyl group onto the aromatic ring reduces interaction between the chromophores and enhances the probability of emission.

The fluorescence spectrum of 1-Et in MTHF at 77 K (Figure 2) bears little resemblance to the emission spectrum of the monomer and shows an enhanced emission of the 0,1 band, most likely from excimers formed between closely spaced chromophores. However, such interactions must be weak, since the emission spectrum does not show a large red shift and the excitation spectrum is identical with that for 4-Et and is independent of the monitoring wavelength.

The 0,0 emission band of 1-Et in MTHF at 77 K is much less intense than that of 1-H. There are two possible

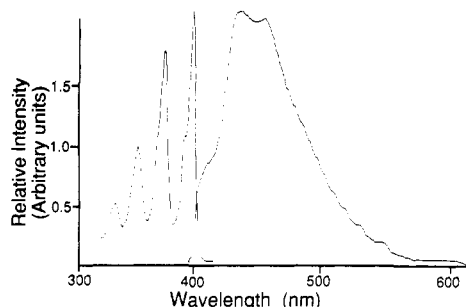


Figure 2. Excitation (left) and emission (right) spectra of 1-Et in 2-methyltetrahydrofuran (ca. 10^{-3} M) at 77 K. Excitation at 380 nm and emission monitored at 520 nm.

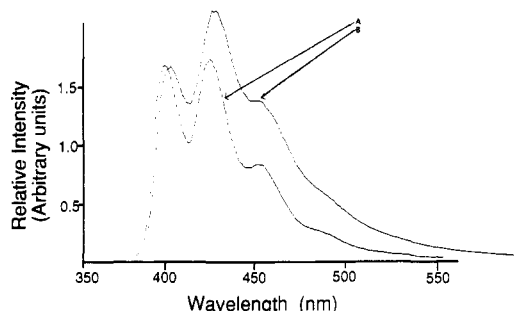


Figure 3. Fluorescence spectra of 2-*i*-Pr (A) and 1-*i*-Pr (B) in benzene (ca. 10^{-3} M) under nitrogen. Excitation at 380 nm.

rationales for this behavior: (1) the excitation energy migrates through the polymer until it is trapped at a preformed excimer site, i.e., at a potential energy minima on the excited-state surface; or (2) the interactions between the chromophores in 1-H are so strong that its excimer fluorescence is strongly quenched, while in 1-Et the interactions would be weaker and excimer emission more favorable. Although these mechanisms cannot now be distinguished, it is likely that both processes are operating since energy migration and excimer formation can be viewed as competing processes.

(3) **1-*n*-Bu.** The fluorescence spectrum of 1-*n*-Bu is similar to that of 1-Et except that excimer emission is not as pronounced: $I_D/I_M = 2.26$, i.e., $\approx 20\%$ lower. The excimer emission maximum is blue-shifted ca. 10 nm from 1-Et, indicating that the butyl group destabilizes the excimer. In MTHF, I_D/I_M increases to 2.5, implying that excimer formation along the polymer chain has become more favorable. The intensity of excimer emission can also be increased by the addition of a polar (methanol) or non-polar (hexane) additive. Thus, changes in the excimer intensity with solvent result from chain contraction and not from alteration in the polarity or dielectric constant of the solvent.

The fluorescence spectrum of 1-*n*-Bu in MTHF at 77 K is better resolved than that of 1-Et, suggesting either that there are fewer preformed excimer sites or that energy migration to these sites is not as favorable. As before, its excitation spectra resembles that of the corresponding pivalate and is independent of monitoring wavelength.

(4) **1-*i*-Pr.** The fluorescence spectrum of 1-*i*-Pr more closely resembles that of its copolymer 2-*i*-Pr (Figure 3). The emission maximum of 1-*i*-Pr is red-shifted ca. 4 nm from 2-*i*-Pr and there is enhanced emission at longer wavelengths. The increased intensity of the 0,1 band of the homopolymer relative to the copolymer implies that 1-*i*-Pr can form weak intramolecular excimers between adjacent chromophores. The fluorescence spectrum is not dramatically different in MTHF and benzene, which signifies that the isopropyl substituent hinders intramo-

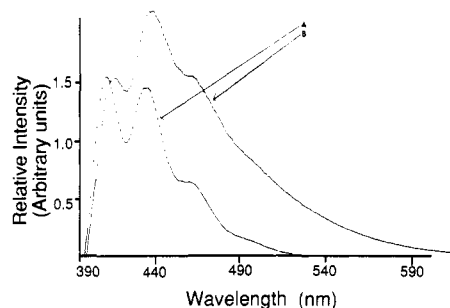


Figure 4. Fluorescence spectra of 2-Ph (A) and 1-Ph (B) in benzene (ca. 10^{-3} M) under nitrogen. Excitation at 380 nm.

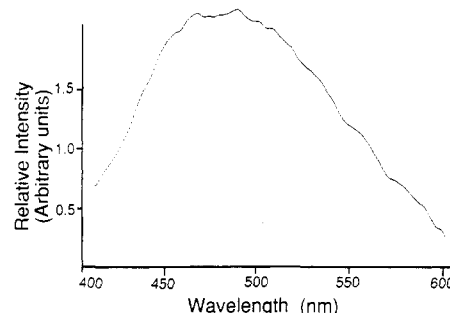


Figure 5. Fluorescence spectrum of a thin film of 1-H on glass under argon. Excitation at 380 nm.

lecular interactions in both solvents. The fluorescence quantum yield of 1-*i*-Pr is ca. 10% smaller than that of 2-*i*-Pr. Therefore, excimer formation does not significantly enhance fluorescence quenching but it is not known whether intersystem crossing or internal conversion is enhanced.

The emission spectrum of 1-*i*-Pr in MTHF at 77 K is a mirror image of the excitation spectrum, with the 0,0 band most intense. The concentration of preformed excimer sites must be very small since the steric bulk of the substituent prevents close approach of the chromophores. However, the fluorescence maxima are red-shifted 4 nm from those of 2-*i*-Pr and the vibrational bands are broader, indicating weak chromophore interactions.

(5) **1-Ph.** The fluorescence spectrum of 1-Ph is similar to that of 2-Ph (Figure 4), except the monomer bands are red-shifted 5 nm, the intensities of the vibrational bands differ, and the spectrum tails further to the red with loss of vibrational resolution. The spectral tailing is indicative of excimer formation: over 50% of the emission of 1-Ph can be attributed to excimer. This is surprising, since excimer emission was not observed in bis(2-(10-phenyl-9-anthryl)ethyl) glutarate⁷ by steady-state fluorescence measurements. The fluorescence spectrum is not dramatically different in MTHF, indicating that excimer formation occurs between nearest neighbors. The quantum yield of fluorescence is reduced ca. 10% from that of the copolymer, which is consistent with a lack of significant fluorescence quenching via excimer formation.

The fluorescence spectrum of 1-Ph in MTHF at 77 K is a mirror image of the excitation spectrum, implying that excimer formation is a dynamic process and that preformed excimer sites are not present. The Stokes shift in the polymer is much larger than that observed for the analogous glutarate, indicating that the polarities of the two environments are different.¹⁸

B. In Thin Films. A typical fluorescence spectrum of a thin film of 1-H spin-coated onto glass slides is shown in Figure 5. Such spectra are characterized by broad, structureless red-shifted emission in which monomer fluorescence is completely absent. In 1-H, this emission is

centered around 490 nm, which is blue-shifted 35 nm from that observed in solution. This emission is very weak, indicating that strong fluorescence quenching has occurred. The fluorescence spectrum of a thin film of 1-Et resembles the solution-phase spectrum, except that the second emission band at 529 nm is blue-shifted by ca. 30 nm and its intensity is reduced. A distinct excimer band is absent for a thin film of 1-*n*-Bu and its fluorescence spectrum exhibits only a single maximum at 458 nm, tailing to 600 nm. The fluorescence spectra of 1-*i*-Pr and 1-Ph are almost identical, with no structured emission and with maxima at 455 nm.

The excitation spectra of the homopolymers 2 are red-shifted 1–2 nm in the film. Similar small spectral shifts ($<250\text{ cm}^{-1}$, $\approx 3.5\text{ nm}$) for anthracene absorbed on silica gel¹⁹ have been attributed to weak interactions (dispersion forces) between the support and the aromatic adsorbate, which stabilizes the excited state more than the ground state.²⁰

C. Delayed Fluorescence. In dilute ($\approx 5 \times 10^{-6}\text{ M}$) solutions of MTHF at 77 K, the homopolymers 1 exhibit delayed monomer and excimer fluorescence. The accepted mechanism for p-type delayed fluorescence is through triplet-triplet annihilation.¹⁴ However, in a rigid medium, diffusion of the chromophores is inhibited. In polymers of high molecular weight with chromophores with long-lived triplet states, there is a finite probability of having two excited chromophores on the same chain: triplet energy can hop from chromophore to chromophore through electron-exchange interaction (Dexter mechanism). In poly(2-vinylnaphthalene)²¹ and poly(*N*-vinylcarbazole)²² at 77 K, the ratio of delayed fluorescence to phosphorescence increased with the molecular weight of the polymer, suggesting that delayed fluorescence in thin films can occur through energy migration through a single polymer chain.

The delayed fluorescence spectrum of 1-H exhibits only excimer emission with at $\lambda = 524\text{ nm}$, which is similar to that found in the solution-phase spectrum ($\lambda = 525\text{ nm}$). No additional emission was observed from 680 to 900 nm. Thus, triplet energy probably hops along a chain until it encounters a low-energy trap. This will localize the triplet energy until it decays or encounters another triplet state.

The delayed fluorescence spectra of the 10-substituted 1 show a decrease in excimer fluorescence and an increase in monomer fluorescence with substituent size. The delayed fluorescence spectrum of 1-Et is dominated by excimer emission but there is a small shoulder attributed to monomer emission at 409 nm. This spectrum is very similar to the prompt fluorescence spectrum of 1-Et at 77 K, indicating that singlet energy migration might also occur. The delayed fluorescence spectrum of 1-*i*-Pr shows an increase in monomer fluorescence but the spectrum is still dominated by excimer emission at 515 nm. The delayed fluorescence spectrum of 1-Ph has approximately equal contributions from monomer and excimer fluorescence. The prompt fluorescence spectra of 1-Ph and 1-*i*-Pr in rigid glasses do not show excimer emission, while the delayed fluorescence spectra do contain excimer emission.

Fluorescence Decay. A. Solution Phase. The fluorescence decay of each polymer was measured by single-photon counting in degassed benzene at the 0,0 band for the monomer and at a wavelength at which only the excimer emits (typically 550–590 nm) on two different time scales (50 ns and 200 or 400 ns). The best fit for the monomer decay functions⁷ of 1 is compared with those of 2 and 4 in Table V. The monomer fluorescence decays of 1 are characterized by a sum of exponentials (if delayed fluorescence is ignored) much like that reported previously

Table V
Fluorescence Lifetimes of Monomer Components of 1, 2, and 4 in Dilute Benzene^{a,b}

subst	τ_F , ns (A) ^c		τ_F , ns		λ , ^d nm
	1	1	2	4	
H ^e	20 (0.24)	5.6 (0.76)	7.1	7.6	395
Et	17 (0.07)	3.0 (0.93)	11	11	411
<i>n</i> -Bu	16 (0.19)	3.2 (0.81)	11	11	411
<i>i</i> -Pr	19 (0.61)	3.2 (0.39)	11	11	412
Ph	31 (0.48)	2.7 (0.52)	8.6	8.6	411

^a Nitrogen-saturated solutions at room temperature. ^b All measurements repeated 3–6 times. Error $\pm 10\%$. ^c From $i(t) = \sum A_i e^{-t/\tau_i}$. ^d Monitoring wavelength. ^e High molecular weight fraction.

Table VI
Fluorescence Lifetimes of Excimer Components of Homopolymers 1 in Dilute Benzene^{a,b}

subst	τ_F , ns (A) ^c		λ , ^d nm
	1	1	
H ^{e,f}	34 (0.34)	18 (0.66)	550
Et	230 (0.26)	85 (0.74)	590
<i>n</i> -Bu	210 (0.44)	17 (0.56)	590
<i>i</i> -Pr	86 (0.85)	18 (0.15)	560
Ph	60 (0.44)	24 (0.56)	560

^a Nitrogen-saturated solutions at room temperature. ^b All measurements repeated 3–6 times. Error $\pm 10\%$. ^c From $i(t) = \sum A_i e^{-t/\tau_i}$. ^d Monitoring wavelength. ^e High molecular weight fraction. ^f A third 6.0-ns component ($A = 0.59$) may be an artifact of the fitting routine.

for the substituted glutarates.⁷ Since the lifetimes of the long-lived components are longer than those of the unquenched monomers, it probably arises from the dissociation of the excimer. The short-lived component could represent the quenched monomers.

Analogous observations have been made with 1-vinylnaphthalene-methyl methacrylate copolymers,²³ where transient decays of the monomer could be fit to a sum of three exponentials. One component is associated with the dissociation of the excimer, while the other two components were associated with a quenched monomer involved in excimer formation and an isolated chromophore that could populate an excimer through energy migration or through segmental diffusion of the polymer chain. As the mole fraction of naphthalene moieties increased, the lifetimes of the monomers decreased. It was postulated that in a homopolymer the short-lived component would not be observed in a nanosecond time scale experiment and the biexponential decay would approximate the excimer lifetime and the weighted average of the two monomer lifetimes.

This situation appears also to occur in 1-H. The solvent-dependent fluorescence spectra suggest that isolated monomer units are present, and the observed lifetime of the monomer component of 1-H is longer than that reported for glutarate 4 ($1/\lambda_2 = 3.5\text{ ns}$).⁷ This increase in monomer lifetime suggests a reduction in fluorescence quenching from excimer formation but this is not consistent with the fivefold reduction in Φ_F for 1-H (cf. 2-H, Table IV). Therefore, two distinct emissive isolated chromophores are present in 1-H, as has been suggested to explain the fluorescence decays of poly(2-naphthylalkyl methacrylates).¹⁰

The fluorescence decay of the excimer of high molecular weight 1-H monitored at 550 nm exhibited two lifetimes similar to those observed in the isolated chromophore (Table VI). Although τ_1 is very similar to the decay of the monomer, no rise time was associated with this or any other component of the decay. This indicates that excimer formation is so fast that it is beyond the detection limits

of the experiment (<1 ns) and/or that there are performed excimer sites in the polymer such that the concentration of excimer is nonzero at the instant of excitation. This also suggests that τ_1 arises from a quenched excimer. The decay of τ_2 is very similar to the long-lived component of the monomer decay ($\tau = 20$ ns) and most likely they are related (excimer/dissociated excimer). The observation of two different excimer decays for 1-H is in agreement with the steady-state fluorescence spectra which implicated two excimers: (1) a strained excimer between adjacent chromophores and (2) a nonstrained excimer between different segments of the polymer chain. Since the excimers are expected to have different geometries, they will decay at different rates.

The fluorescence decays of the 10-substituted 1 monitored at the 0,0 band of the monomer could be fit to the sum of two exponentials which arise from a quenched monomer and a dissociated excimer. For 1-Et and 1-*n*-Bu, there should be two monomeric species with different lifetimes since the solvent-dependent fluorescence spectra indicate that there are two excimers. Evidently, the two components cannot be resolved. Although steric hindrance of the bulky substituents in 1-*i*-Pr and 1-Ph might prevent rapid excimer formation, rapid fluorescence quenching may occur at sites that possess an appropriate geometry for excimer formation.

Two excimer decays are also expected from 1-Et and 1-*n*-Bu. However, these components might be difficult to isolate from the monomer emission, since the excimer emission for the analogous glutarates could not be completely isolated from monomer emission for the strained excimer.⁷ The excimer emissions for 1-*n*-Bu and 1-*i*-Pr measured on a long time scale contain a component with a lifetime similar ($\pm 10\%$) to a component in the monomer decay. This is expected in a system that contains a monomer/excimer equilibrium. The excimer emission for 1-*n*-Bu was also measured on a short time scale (50 ns) to investigate short-lived components. Surprisingly, the fluorescence intensity decayed less than 5% over the experimental time scale. A rise time of 1.8 ns was observed, as is consistent with rapid excimer formation.

Thus, the fluorescence decays of the homopolymers are complex. The monomer decays could be described by a sum of two exponentials indicative of a simple monomer/excimer equilibrium. However, a short (subnanosecond) lifetime is expected for excimer formation between nearest neighbors. Substitution appears to have very little effect on the calculated lifetimes.

The decays of the excimer emission contained a component (15–35 ns) that was also present in the monomer emission, supporting the hypothesis of a monomer/excimer equilibrium. The excimer decays were complicated by the contribution of delayed excimer fluorescence which, although it could be reduced by using low molecular weight polymers or by adding small quantities of a triplet quencher, made further interpretation risky.

B. Films. The transient fluorescence decays of thin films of the homopolymers 1 ($OD < 0.15$) cast on SnO_2 plates were measured under argon (Table VII). These could also be fit to a sum of three exponentials: quenched monomer, excimer emission, and a third unidentified (minor) long-lived component. On a long time scale (200 or 400 ns), the third component did not significantly decay. The monomer and excimer lifetimes in the films are shorter than the lifetimes in dilute benzene. In films, inter- and intrapolymer chain excimers can form. The fluorescence spectra of the films did not show a long-wavelength ex-

Table VII
Fluorescence Decay Parameters for Spin-Coated Films of 1

subst	$\lambda, ^\circ \text{nm}$	$\tau_1, \text{ns (A)}^d$	$\tau_2, \text{ns (A)}$	$\tau_3, \text{ns (A)}$
H ^a	460	2.5 (0.64)	16 (0.30)	72 (0.14)
Et ^a	468	2.1 (0.57)	8.4 (0.36)	54 (0.07)
<i>n</i> -Bu ^a	458	3.1 (0.69)	12 (0.25)	67 (0.07)
Ph	460	3.0 (0.57)	9.3 (0.40)	33 (0.03)

^a Spin-coated on SnO_2 , $OD < 0.15$, under argon. ^b Spin-coated on glass, $OD < 0.15$, under argon. ^c Monitoring wavelength. ^d From $i(t) = \sum A_i e^{-t/\tau_i}$.

cimer emission ($\lambda \approx 550$ nm) except in 1-Et, which shows a second maximum at longer wavelengths and a shorter monomer and excimer lifetime than 1-*n*-Bu. The loss of monomer structure in the emission spectra and the decrease in the fluorescence lifetimes imply that energy migrates to excimer-forming sites. Thus, similar structural features emerge from a consideration of the steady-state and time-resolved fluorescence of the films.

Fluorescence Quenching and Singlet Energy Migration in Solution. The occurrence of energy migration is established by comparing the rate constants for fluorescence quenching by an appropriate chemical probe of the homopolymers 1 to those of copolymers 2 or the monomeric model compounds (substituted pivalates 4). An increase in quenching in the homopolymers 1 is interpreted as a consequence of energy migration. Experimentally, the rate constants for quenching are determined from changes in the lifetime of the singlet excited state and the change in the intensity of fluorescence as a function of quencher concentration.

The fluorescence quencher should be an efficient collisional quencher ($k_Q \approx k_{\text{Diff}}$) that does not form a ground-state complex or chemically react with the ground- or excited-state chromophore. The quencher must also be sufficiently small so that diffusion into a coiled polymer chain can occur without serious steric inhibition. A molecule that fits these requirements is nitromethane. It has been shown to efficiently quench the fluorescence of 9,10-diphenylanthracene ($k_Q = 4.3 \times 10^9 \text{ M}^{-1} \text{ s}^{-1}$)²⁴ in cyclohexane without forming any new spectroscopic states or products. Its only disadvantage is that its absorption band ($\lambda_{\text{max}} = 271$ nm, $\epsilon = 18.6 \text{ M}^{-1} \text{ cm}^{-1}$) tails into the region where the chromophores are excited ($\lambda = 380$ nm, $\epsilon < 0.05 \text{ M}^{-1} \text{ cm}^{-1}$). Therefore, the anthracene moieties were excited at wavelengths longer than 380 nm and the concentration of quencher was kept low (<0.2 M) to avoid competitive light absorption by the quencher (OD of samples typically <0.05). In addition, the concentration of quencher should be kept low to avoid changing the conformation of the polymer in solution (in case the quencher acts as a nonsolvent), which would cause deviations in the predicted fluorescence behavior.

In order to interpret the results from the fluorescence quenching experiments, a kinetic model is required to describe the collisional quenching of the monomer/excimer system. The intramolecular interactions of a bi-chromophore system have been described⁷ by the simple kinetic scheme derived by Birks²⁵ for intermolecular excimer formation (Appendix).

Johnson²⁶ has described a modification of this scheme to describe the transient decay of poly(*N*-vinylcarbazole) in which an additional term k_{EFD} is added to the rate of excimer formation k_{DM} , where k_{E} represents the rate of energy transfer and f_{D} represents the fraction of preformed excimer sites. This will account for $[^1\text{D}^*] \neq 0$ immediately after the excitation pulse. It has been shown that f_{D} is 10^{-2} for thin films of poly(2-vinylnaphthalene) and 10^{-3} for thin films of polystyrene.^{27,28} Therefore, in

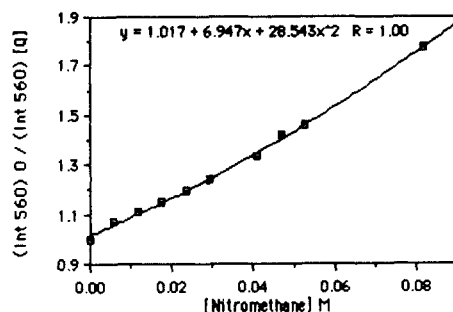


Figure 6. Stern-Volmer plot for excimer fluorescence quenching (monitored at 560 nm) of 1-Et by nitromethane.

a good polymer solvent (chain expanded), it can be assumed that $f_D \ll 1$ and the kinetic scheme is reduced back to that described by Birks.²⁵ We therefore assume (1) k_{DM} describes a weighted average of all the conformations leading to excimer formation from adjacent and nonadjacent chromophores and (2) the rate of singlet energy migration can be combined into k_{DM} since energy migration most likely will occur until it is caught by a trap, i.e., an excimer-forming site.

With nitromethane as quencher, the ratios of the fluorescence intensities do not follow a simple Stern-Volmer relation. These equations can be simplified if the rate of excimer dissociation k_{MD} is slow compared to the rate of deactivation of the excimer k_D . A comparison between the excimer of the bichromophore and the polymer can be made, since the stabilization and the deactivation pathways should be similar. This was found to be true for poly(2-vinylnaphthalene) (PVN) and 1,3-bis(2-naphthyl)propane (BNP) in which the energy of activation for excimer dissociation was calculated to be very similar (PVN: $E_a^{DM} = -8.5$ to -10.0 kcal mol⁻¹;^{29,30} BNP: $E_c = 9.7$ kcal mol⁻¹ ^{31,32}). Therefore, it is reasonable to assume that

$$(k_M + k_{DM})(k_D + k_{MD}) \gg k_{MD}k_{DM}$$

The quenching of monomer fluorescence can then be reduced to the simple Stern-Volmer relationship

$$I_M/I_{QM} = 1 + k_{QM}\tau_M[Q]$$

where $\tau_M (=k_M + k_{DM})$ is the lifetime of the monomer.

The intensity of monomer emission for the homopolymers in the presence and absence of quencher I_M/I_{QM} measured at the 0,0 band was plotted against the concentration of quencher. The plots are linear for 1-Et and 1-*n*-Bu while those for 1-*i*-Pr and 1-Ph are nonlinear. The intensity of the monomer emission of 1-H remained constant up to 0.13 M nitromethane. Higher concentrations of quencher could not be employed since the optical density of the nitromethane was ca. 10% that of the homopolymer.

Plots of I_D/I_{QD} against concentration of quencher for 1-Et, 1-*n*-Bu, 1-*i*-Pr, and 1-Ph (Figure 6) show upward curvature that can be described by a quadratic. A similar plot for 1-H is linear, but this is expected since $k_{QM} \approx 0$. A plot of the ratio of excimer-to-monomer fluorescence against quencher concentration for 1-Et and 1-*n*-Bu was found to be linear, while the ratio of excimer-to-monomer fluorescence for 1-*i*-Pr and 1-Ph remained constant.

The results from the quenching study show that the assumptions made in the derivation of the equations were valid for 1-Et and 1-*n*-Bu but not for 1-*i*-Pr and 1-Ph. The absence of monomer quenching for 1-H probably indicates that the polymer chain is folded such that monomer units are isolated from the bulk of the solvent (and quencher).

However, quenching of the excimer fluorescence adheres to the predicted theory if $k_{QM} \approx 0$. The assumption $k_{MD}k_D^{-1} \ll 1$ may not be valid for 1-*i*-Pr and 1-Ph, since bulky substituents hinder interaction between the chromophores and favor dissociation of the excimer, as was found for the glutarates in which k_{MD}/k_{DM} increased with substitution.⁷ A similar upward curvature in the plot of I_M/I_{QM} against quencher concentration was found for atactic poly(*o*-methylstyrene), while the meta and para isomers gave linear plots.³³

The observed Stern-Volmer quenching constants ($K_{SV} = k_{QM}\tau_M$) of the homopolymers 1 are listed in Table VIII. The monomer quenching constants for 1-*i*-Pr and 1-Ph were estimated from the initial slopes of Stern-Volmer plots. The Stern-Volmer quenching constants for the excimer ($K_{SV})_D$ of 1-Et and 1-*n*-Bu were determined by two methods: (1) from the slopes of the plots of eq 9 and (2) by subtraction of ($K_{SV})_M$ from the first-order term [$(K_{SV})_M + (K_{SV})_D$].

The rate constants for quenching of the homopolymers can be determined from ($K_{SV})_M$ and the lifetime of the singlet state. However, the decay of the monomer emission of the homopolymers was biexponential. One method to characterize the decay functions is to define a "mean duration" (τ_M) of the emission³⁴ which represents a weighted average of the lifetimes.³⁵ Since this method takes into account the dissociation of the excimer, it is the preferred method for determining k_{QM} from the change in the transient decay as a function of quencher concentration. Although this method (τ_M against $[Q]$) provides a more accurate description of the quenching rates (compared with measuring the fluorescence intensities), it was deemed unsatisfactory for the homopolymers as a consequence of short monomer lifetimes and the experimental difficulties associated with accurately measuring small changes in a multiexponential decay function.

The rate constants for quenching the excimer fluorescence (Table VIII) were calculated from ($K_{SV})_D$ and the lifetime of the excimer emission. These rates are ca. 1 order of magnitude slower than the quenching rates of the monomer emission. This could result from a decrease in the accessibility of the quencher to the chromophores or a reduced quenching probability per collision. The rate constant for quenching of the excimer fluorescence of polystyrene with CCl₄ is also smaller than that for the monomer emission of polystyrene or for ethylbenzene,³⁵ suggesting that this is a general phenomenon.

The plots of I/I_Q against quencher concentration for the copolymers 2 and the pivalates 4 were linear. The observed Stern-Volmer quenching constants ($K_{SV} = k_{QM}\tau_M$) for the copolymers and pivalates 4 are shown in Table IX. There is a good agreement between the rate constants for fluorescence quenching, indicating that the methacrylate backbone of the polymer does not impose steric restrictions to approach of the quencher.

The rate constants for quenching of the monomer fluorescence k_{QM} of 1-Et and 1-*n*-Bu are similar, within experimental error ($\pm 10\%$), to those of the corresponding copolymers 2, while k_{QM} of 1-*i*-Pr and 1-Ph are much larger than their corresponding copolymers. This indicates that another factor besides quencher diffusion is involved. Although fluorescence quenching probably occurs through an exciplex (the reduction potential for nitromethane is ca. 1 V below the LUMO of the substituted anthracene³⁶), there should not be preferential complexation of the quencher to a ground-state anthracene giving rise to static quenching. All the substituted anthracenes have similar reduction and oxidation potentials and, as a consequence

Table VIII
Fluorescence Quenching of 1^a

subst	(<i>K</i> _{SV}) _M , M ⁻¹	<i>k</i> _{QM} × 10 ⁻⁹ , M ⁻¹ s ⁻¹	(<i>K</i> _{SV}) _{D1} , M ⁻¹	(<i>K</i> _{SV}) _{D2} , M ⁻¹	<i>k</i> _{QD} × 10 ⁻⁸ , M ⁻¹ s ⁻¹	Λ × 10 ⁴ , cm ² s ⁻¹	<i>L</i> , Å
H ^b			9.1 ^c		5.0	0	
Et	6.0	2.0	1.0	1.5	0.58	0	
<i>n</i> -Bu	6.0	1.9	4.6	6.5	3.0	0	
<i>i</i> -Pr	44 ^c	14	44 ^d		24	1.8	100
Ph	21 ^c	7.7	21 ^d		6.6	6.6	83

^a Calculated as described in the Appendix. ^b High molecular weight fraction. ^c Estimated from initial slope of *I*_M/*I*_{QM}. ^d Estimated from initial slope of the plot.

Table IX
Fluorescence Quenching of 1 and 2 with Nitromethane

subst	1		2	
	<i>K</i> _{SV} , ^a M ⁻¹	<i>k</i> _{QM} × 10 ⁻⁹ , M ⁻¹ s ⁻¹	<i>K</i> _{SV} , ^a M ⁻¹	<i>k</i> _{QM} × 10 ⁻⁹ , M ⁻¹ s ⁻¹
H	34	4.4	23	3.2
Et	31	2.8	25	2.3
<i>n</i> -Bu	28	2.6	25	2.3
<i>i</i> -Pr	21	1.9	26	2.4
Ph	18	2.1	15	1.8

^a Error ±10%.

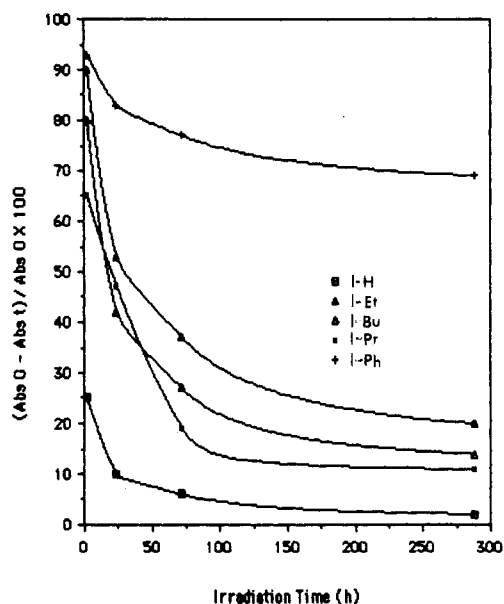


Figure 7. Fractional photobleaching of polymers 1 in degassed benzene (ca. 10⁻⁴ M) with irradiation time. Incident wavelengths longer than 330 nm. Chromophore disappearance monitored at the polymer's absorption maximum.

of the steric bulk of the isopropyl and phenyl substituents, the polymer chains should be quite extended. Therefore, the enhanced quenching must be a consequence of singlet energy migration.

The diffusion length *L* of the excitation energy through the polymer can be estimated from the Smoluchowski-Einstein relationship and the estimated diffusion coefficient for nitromethane in benzene.³⁷ The results in Table VIII show that singlet energy migration is significant for 1-*i*-Pr and 1-Ph. If the average nearest-neighbor separation between chromophores is assumed to be 8–9 Å (from MM2 calculations of the unsubstituted glutarate),⁷ then there are an average of 9–13 hops of the excitation energy within the lifetime of the excited state.

Photostability. A plot of the change in absorbance with irradiation time for the homopolymers 1 is shown in Figure 7. All suffer some decomposition. 1-H decomposes under irradiation much faster than 3-H,⁷ with only 25% of the initial chromophores remaining after 2 h of irradiation. Similar behavior has been reported for poly(9-anthryl-

methyl methacrylate) in which the quantum yield of disappearance was 0.01,³⁸ while bis(9-anthrylmethyl) succinate, a monomeric model for the polymer, the quantum yield of disappearance was 0.015 in dilute solution. The enhanced decomposition of the polymer was attributed to the reduced conformational mobility of the chromophores since the quantum yield of disappearance of the succinate doubled when attached to a polymer backbone.³⁹

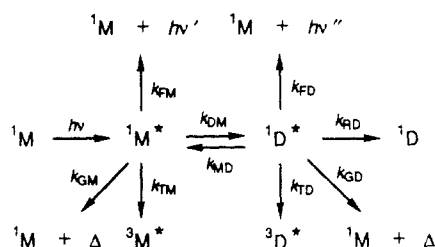
The products of the photodecomposition have not been determined but they are likely to arise from photochemical cross-linking. In the photodecomposition of poly(9-anthrylmethyl methacrylate), for example, products derived from cleavage of the anthryl group from the backbone were isolated.³⁸ GPC analysis of the photoproducts from 1-H, in contrast, revealed no low molecular weight fractions. The isolated insoluble material indicated cross-linking, since intramolecular reactions should dominate at the low concentrations of the irradiation (10⁻⁴ M). By analogy with 3-H,⁷ this photoreactivity is likely to involve head-to-tail dimerization of the anthryl groups. Heating a benzene solution of the decomposed polymer at 290 °C for 3 h in a sealed tube resulted in a restoration of 21% of the original intensity of the anthryl absorption, as would be expected for a thermal reversion of the photodimers.⁷

Conclusions

Thus, interchromophore interactions in the homopolymers 1 were sensitive to the bulk of a substituent at the 10-position of the anthryl ring. These effects could be clearly seen in relative fluorescence yields and lifetimes in the series, in the relative contributions of fluorescence from isolated chromophores and interactive excimers, and in the relative intensity of delayed fluorescence in the polymers occurring via triplet energy migration to preformed traps. Those homopolymers that exhibit significant fluorescence quenching, compared to their model compounds, do not show energy migration, while those showing only minimal fluorescence quenching (i.e., those with a bulky substituent) exhibit energy migration. Excimer formation competes with energy migration and functions as a low-energy trap. Similar results were found for poly(9-anthrylmethyl methacrylate) and poly((10-phenyl-9-anthryl)methyl methacrylate),³⁸ in which energy migration was found only for the phenyl-substituted derivative. Therefore, in excimer-forming polymers, there is a delicate balance between the distance and geometry of the chromophores necessary to maximize energy migration but minimize excimer formation, a conclusion that has also been reached in studies of poly(2-vinylnaphthalene) and poly(2-*tert*-butyl-6-vinylnaphthalene) having a small fraction of 2-vinylnaphthalene copolymerized into the polymer chain as a fluorescent energy trap.⁴⁰ This payoff of effects is critical in attempts to correlate polymer structure with sensitization efficiency in polymeric layers.

Acknowledgment. This work was supported by the Office of Basic Energy Sciences, Fundamental Interactions Branch, Division of Chemical Sciences, of the U.S. Department of Energy.

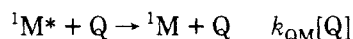
Scheme I
Kinetic Scheme for Intramolecular Excimer Formation^{8,26}



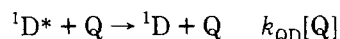
Appendix I

To apply Birk's kinetic scheme^{8,25} to fluorescence quenching by a collisional quencher, two more processes must be included in Scheme I:

Quenching of the monomer:



Quenching of the excimer:



The photostationary concentration of the emitting species in the absence of quencher, $[^1M^*]$ and $[^1D^*]$, and in the presence of quencher, $[^1M^*]_Q$ and $[^1D^*]_Q$ can then be written as

$$[^1M^*] = \frac{I_a(k_D + k_{MD})}{(k_M + k_{DM})(k_D + k_{MD}) - k_{MD}k_{DM}} \quad (1)$$

$$[^1M^*]_Q = [I_a(k_D + k_{MD} + k_{QD}[Q])]/[(k_M + k_{DM} + k_{QM}[Q])(k_D + k_{MD} + k_{QD}[Q]) - k_{MD}k_{DM}] \quad (2)$$

$$[^1D^*] = \frac{I_a k_{DM}}{(k_M + k_{DM})(k_D + k_{MD}) - k_{MD}k_{DM}} \quad (3)$$

$$[^1D^*]_Q = I_a k_{DM}/[(k_M + k_{DM} + k_{QM}[Q])(k_D + k_{MD} + k_{QD}[Q]) - k_{MD}k_{DM}] \quad (4)$$

where I_a is the rate of light absorption. The ratio of the intensity of the monomer emission $I_M (=k_{FM}[^1M^*])$ in the absence and presence of quencher I_{QM} is

$$I_M/I_{QM} = \{k_{FM}I_a(k_D + k_{MD})[(k_M + k_{DM} + k_{QM}[Q])(k_D + k_{MD} + k_{QD}[Q]) - k_{MD}k_{DM}]\}/\{k_{FM}I_a[(k_M + k_{DM})(k_D + k_{MD}) - k_{MD}k_{DM}]\} \quad (5)$$

which can be simplified to

$$\frac{I_M}{I_{QM}} = \frac{k_D + k_{MD}}{(k_M + k_{DM})(k_D + k_{MD}) - k_{MD}k_{DM}} \left[k_M + k_{MD} + \frac{k_{MD}k_{DM}}{k_D + k_{MD} + k_{QD}[Q]} \right] \quad (6)$$

The ratio of the intensities of excimer emission $I_D (=k_{FD}[^1D^*])$ in the absence and presence of quencher I_{QD} can be written as

$$\frac{I_D}{I_{QD}} = \frac{(k_M + k_{DM} + k_{QM}[Q])(k_D + k_{MD} + k_{QD}[Q]) - k_{MD}k_{DM}}{(k_M + k_{DM})(k_D + k_{MD}) - k_{MD}k_{DM}} \quad (7)$$

The relationship for quenching of the excimer emission in eq 7 can be simplified as follows:

$$I_D/I_{QD} = 1 + (\tau_M k_{QM} + \tau_D k_{QD})[Q] + (\tau_M k_{QM})(\tau_D k_{QD})[Q]^2 \quad (8)$$

where $\tau_D (=k_D + k_{MD})$ is the lifetime of the excimer if the rate of excimer dissociation is small compared to its deactivation. The rate constant for quenching of the excimer k_{QD} can be determined as

$$\frac{I_D/I_{QD}}{I_M/I_{QM}} = 1 + k_{QD}\tau_D[Q] \quad (9)$$

References and Notes

- Gerischer, H.; Willig, F. *Top. Curr. Chem.* **1976**, *61*, 31.
- Desilvestro, J.; Grätzel, M.; Kavan, L.; Moser, J.; Augustynski, J. *J. Am. Chem. Soc.* **1985**, *107*, 2988. (b) Vlachopoulos, N.; Liska, P.; Augustynski, J.; Grätzel, M. *Ibid.* **1988**, *110*, 1216.
- Fox, M. A.; Britt, P. F. *J. Phys. Chem.* **1990**, *94*, 6351.
- Melhuish, W. H. *J. Phys. Chem.* **1961**, *65*, 229.
- O'Connor, D. V.; Phillips, D. *Time Correlated Single Photon Counting*; Academic Press: New York, 1984.
- Tazuke, S.; Hayashi, N. *Polym. J.* **1978**, *10*, 443.
- Fox, M. A.; Britt, P. F. *Photochem. Photobiol.* **1990**, *51*, 129.
- Birks, J. B. *Prog. React. Kinet.* **1970**, *5*, 181.
- Holden, D. A.; Wang, P. Y. K.; Guillet, J. E. *Macromolecules* **1980**, *13*, 295.
- Aspler, J. S.; Guillet, J. E. *Macromolecules* **1979**, *12*, 1082.
- Nishijima, Y.; Mitani, K.; Katayama, S.; Yamamoto, M. *Rep. Prog. Polym. Phys. Jpn.* **1970**, *13*, 421.
- Fitzgibbon, P. D.; Frank, C. W. *Macromolecules* **1982**, *15*, 733.
- (a) Torkelson, J. M.; Lipsky, S.; Tirrell, M. *Macromolecules* **1981**, *14*, 1603. (b) Lindsell, W. E.; Robertson, F. C.; Soutar, I. *Eur. Polym. J.* **1981**, *17*, 203.
- Birks, J. B. *Photophysics of Aromatic Molecules*; Wiley-Interscience: London, 1970; Chapter 11.
- This assumes that the polymer chain has not collapsed upon freezing.
- Hargreaves, J. S.; Webber, S. E. *Macromolecules* **1984**, *17*, 235.
- Nakahira, T.; Ishizuka, S.; Iwabuchi, S.; Kojima, K. *Macromolecules* **1983**, *16*, 297.
- Reference 14, p 109.
- Leermaker, P. A.; Thomas, H. T.; Weis, L. T.; James, F. C. *J. Am. Chem. Soc.* **1966**, *88*, 5075.
- Gerischer, H. *Faraday Discuss. Chem. Soc.* **1974**, *58*, 219.
- Pasch, N. F.; Webber, S. E. *Chem. Phys.* **1976**, *16*, 361.
- Klöpffer, W.; Fischer, D.; Nawndorf, G. *Macromolecules* **1977**, *10*, 450.
- Phillips, D.; Roberts, A. J. *J. Polym. Sci., Polym. Phys. Ed.* **1980**, *18*, 2401.
- Delaire, J. A.; Rodgers, M. A. J.; Webber, S. E. *J. Phys. Chem.* **1984**, *88*, 6219.
- Birks, J. B.; Dyson, D. J.; Munro, I. H. *Proc. R. Soc. London* **1963**, *A275*, 575.
- Johnson, G. E. *J. Chem. Phys.* **1975**, *62*, 4697.
- Frank, C. W.; Harrah, L. A. *J. Chem. Phys.* **1974**, *61*, 1526.
- Frank, C. W. *J. Chem. Phys.* **1974**, *61*, 2015.
- Fox, R. B.; Price, T. R.; Cozzens, R. F.; McDonald, J. R. *J. Chem. Phys.* **1972**, *57*, 534.
- David, C.; Putman-de Lavaraille, N.; Gueskens, G. *Eur. Polym. J.* **1977**, *13*, 15.
- Chandross, E. A.; Demster, C. J. *J. Am. Chem. Soc.* **1970**, *92*, 3587.
- Semerak, S. N.; Frank, C. W. *Adv. Polym. Sci.* **1983**, *54*, 33.
- Ishii, T.; Handa, T.; Matsunaga, S. *J. Polym. Sci., Polym. Phys. Ed.* **1979**, *17*, 811.
- (a) Inokut, M.; Hirayama, F. *J. Chem. Phys.* **1965**, *43*, 1978. (b) Ware, W. R. *Chem. Detect. Excited State* **1971**, *1A*, 231.
- Bai, F.; Chang, C. H.; Webber, S. E. *Macromolecules* **1986**, *19*, 588.
- Encyclopedia of Electrochemistry of the Elements*; Bard, A. J., Ed.; Marcel Dekker: New York, 1978; Vol. 13, Chapter 2.
- Gierer, A.; Wirtz, K. *Z. Naturforsch.* **1953**, *8a*, 532.
- Hargreaves, J. S.; Webber, S. E. *Macromolecules* **1984**, *17*, 1741.
- O'Connor, D. V.; Phillips, D. *Time-Correlated Single Photon Counting*; Academic Press: New York, 1984; Chapter 4.
- Nakahira, T.; Sasaoka, T.; Iwabuchi, S.; Kojima, K. *Makromol. Chem.* **1982**, *183*, 1239.